

A B -anomaly motivated Z' boson at the energy and precision frontiers

Ben Allanach^a, Christoph Englert^b, Wrishik Naskar^b

^a*DAMTP, University of Cambridge, Centre for Mathematical Sciences, Wilberforce Road, CB3 0WA, Cambridge, United Kingdom*

^b*School of Physics and Astronomy, University of Glasgow, Kelvin Building, University Avenue, G12 8QQ, Glasgow, United Kingdom*

Abstract

TeV-scale Z' bosons with family-dependent couplings can explain some anomalies inferred from B -meson measurements of processes involving the $b \rightarrow sl^+l^-$ transition. A Z' originating from kinetically-mixed spontaneously broken $U(1)_{B_3-L_2}$ gauge symmetry has been shown to greatly ameliorate global fits [1] in a ‘flavour-preferred’ region of parameter space. We provide an exploration of this region at the high luminosity (HL-)LHC with particular attention to which signals could be verified across different discovery modes. Even if the HL-LHC does not discover the Z' boson in a resonant di-lepton channel, a FCC-ee Z -pole run would detect oblique corrections to the electroweak precision observables (EWPOs). Changes due to Z' -induced non-oblique corrections are unlikely to be detected, to within experimental precision. In any case, the extended discovery potential offered by a 100 TeV pp -collider would afford sensitivity to the entire flavour-preferred region and enable a fine-grained and forensic analysis of the model.

1. Introduction

There exists an interplay between two discovery-led research pillars of the current high-energy particle physics programme: precision flavour investigations which require experimental and theoretical control and searches for

Email addresses: `ben.allanach.work@gmail.com` (Ben Allanach),
`christoph.englert@glasgow.ac.uk` (Christoph Englert),
`w.naskar.1@research.gla.ac.uk` (Wrishik Naskar)

beyond the Standard Model (BSM) states at the highest attainable energies, notably at the Large Hadron Collider (LHC). Searches for new particles in ‘bump-hunt’ analyses do not typically require dedicated experimental and theoretical control; they are data-driven discovery methods. The hypothesis of a certain model BSM can link precision flavour investigations to the search programme (see e.g. [2–6] for similar studies). This not only enables us to make concrete discovery predictions based on observed flavour anomalies but also suggests a multi-faceted exploration programme characterised by checks and balances.

We demonstrate the phenomenological power of such a programme by investigating a concrete model that changes SM predictions for various measurements involving flavour-changing B -meson decays, the malaphoric $U(1)_{B_3-L_2}$ model [1]. In this model, the TeV-scale Z' has interactions with e^+e^- , with $\mu^+\mu^-$ and with $\bar{b}s$ and $\bar{s}b$. It therefore introduces a BSM contribution which interferes with the SM $b \rightarrow sl^+l^-$ amplitude*. Ref. [1] shows that the model ameliorates a SM fit to flavour observables: in a global fit to hundreds of observables, an improvement of 38.2 units of total χ^2 for three effective fit parameters was found. LEP2 di-lepton production constraints on the differential cross-sections, EWPOs and lepton flavour universality constraints are included and are simultaneously well fit.

The lowest hanging fruit of the malaphoric $U(1)_{B_3-L_2}$ model as far as searches are concerned is the bump-hunt search in di-lepton channels [7]; depending upon parameters, this could discover the predicted Z' boson. Here, we build on the search to provide a more comprehensive analysis of the discovery potential at the high-luminosity (HL-)LHC and clarify how combinations of channels with different statistical sensitivity can aid the process of determining the model parameters. In the event that the HL-LHC does not report a discovery of direct Z' production, it will provide a lower limit on the mass of the Z' boson $M_{Z'}$ as a function of g_X , the $U(1)_{B_3-L_2}$ gauge coupling. An emergent question is then whether a potential future precision e^+e^- collider could provide additional sensitivity beyond the direct exclusion constraints established at the LHC. By relying on the underlying model BSM, we can address this question by investigating BSM electroweak corrections, in particular of a precision Z -pole programme.

*We denote l to be a charged lepton in the usual experimental parlance, i.e. either muons or electrons.

We organise this note as follows. In Sec. 2, we briefly sketch salient features of the malaphoric $U(1)_{B_3-L_2}$ model. Specific care is also given to a detailed discussion of rare Z' final states, to inform the discovery projection of the HL-LHC. This is discussed in Sec. 3.1 where we compare the flavour-preferred parameter region with the dominant discovery modes of the model, extending the results of Ref. [1]. Building on the HL-LHC sensitivity prospects for the considered scenario, we turn to precision e^+e^- measurements in Sec. 3.2. Concretely, we investigate helicity asymmetries at one-loop accuracy to navigate the sensitivity of a Z pole programme to the new physics of the malaphoric $U(1)_{B_3-L_2}$ model. We close with conclusions in Sec. 4.

2. The Model

In the malaphoric $B_3 - L_2$ model, the SM is extended by a $U(1)_{B_3-L_2}$ gauge boson, three right-handed neutrino fields and a SM-singlet complex scalar θ with unit $U(1)_{B_3-L_2}$ charge whose vacuum expectation value $v_X \sim \mathcal{O}(\text{TeV})$ spontaneously breaks $U(1)_{B_3-L_2}$. The $U(1)_{B_3-L_2}$ charges of all fields are set to be proportional to[†] third family baryon number minus second family number. The Z' couples to all SM di-fermion pairs via the kinetic mixing parameter ϵ in the Lagrangian

$$\begin{aligned} \mathcal{L}_{XB} = & -\frac{1}{4}X_{\mu\nu}X^{\mu\nu} + g_X^2 X_H^2 |H^\dagger H| X_\mu X^\mu + \frac{1}{2}M_X^2 X_\mu X^\mu \\ & - \frac{\epsilon}{2}B_{\mu\nu}X^{\mu\nu} - X_\mu J^\mu - B_\mu j^\mu, \end{aligned} \quad (1)$$

where $X_{\mu\nu}$ is the $B_3 - L_2$ field strength tensor and $B_{\mu\nu}$ is the hypercharge field strength tensor. $J^\mu = g_X \sum_{\psi'} X_{\psi'} \gamma^\mu \psi'$ is the $B_3 - L_2$ current, where the sum is over the chiral Weyl fermions in the interaction basis ψ' and $X_{\psi'}$ is the $B_3 - L_2$ charge of ψ' (normalised such that the charge of a third-family quarks is +1). j_μ is the hypercharge current, as defined in Ref. [1]. After rotation to the mass eigenbasis of the neutral gauge boson fields $\mathbf{P}_\mu := (A_\mu, Z_\mu, Z'_\mu)^T$, one obtains the following important Lagrangian terms

$$\mathcal{L}_{imp} = -\frac{1}{4}\mathbf{P}_{\mu\nu}^T \mathbf{P}^{\mu\nu} + \frac{1}{2}\mathbf{P}_\mu M_{\mathbf{P}}^2 \mathbf{P}^\mu - \sum_{\psi'} \bar{\psi}' \hat{\mathbf{I}}^T C \mathbf{P} \psi', \quad (2)$$

[†]The constant of proportionality is 3 in order to make all X_ψ integers.

where C is an invertible (but non-unitary) 3 by 3 matrix, $M_{\mathbf{P}}^2 = \text{diag}(0, M_Z^2, M_{Z'}^2)$, and M_Z and $M_{Z'}$ are the physical Z^0 and Z' boson masses, respectively. To a good approximation [7], when $M_Z/M_{Z'} \ll 1$, as is the case here,

$$M_{Z'} = \frac{\sqrt{1 + s_w^2 \epsilon^2}}{\sqrt{1 - \epsilon^2}} M_X, \quad (3)$$

where $s_w = \sin \theta_w$, the sine of the weak mixing angle and we have introduced the three-vector $\hat{\mathbf{I}} := \left(g' Y_{\psi'}, g \hat{L}, g_X X_{\psi'} \right)^T$, where g' is the hypercharge gauge coupling, g the $SU(2)$ gauge coupling, Y_{ψ} is the hypercharge and \hat{L} is an operator that annihilates singlets of $SU(2)_L$ but returns an eigenvalue of $T_3/2$ when acting on left-handed doublet fields. T_3 is the third Pauli matrix.

The Z' has enhanced couplings to di-muons and also to third family quark pairs. Mismatches between the gauge interaction basis and the mass basis of the left-handed strange and left-handed bottom fields mean that an interaction term proportional to $g_X \sin \theta_{sb} \bar{b} \not{Z}' P_L s + H.c.$ is present in the Lagrangian density, where P_L is the left-handed projection matrix for 4-component Dirac fermions. θ_{sb} parameterises the mismatch between the gauge and mass eigenstates of the s_L and b_L fields. With these couplings in place, the Z' mediates an effective interaction $(\bar{b} \gamma_{\mu} P_L s)(\mu^+ \mu^-)$ as well as $(\bar{b} \gamma_{\mu} P_L s)(e^+ e^-)$. New physics contributions to these two operators are preferred [8, 9] by some state-of-the-art estimates of the B -meson decay channel's amplitude [10, 11], although there is debate about whether all SM effects have been adequately accounted for [12]. It was found in Ref. [10] that the best global fit point is $\hat{\epsilon} = -0.92$, $\hat{g}_X = 0.078$ and $\theta_{sb} = -0.17$, where

$$\hat{\epsilon} := \epsilon(3 \text{ TeV})/M_X, \quad \hat{g}_X := g_X(3 \text{ TeV})/M_X \quad (4)$$

\hat{g}_X is in the domain $0.03 - 0.23$ in the 95% confidence level (CL) good-fit region, whereas $\hat{\epsilon}$ is less than -0.1 [1]. Direct Z' production signatures at colliders are insensitive to the value of θ_{sb} to a good approximation [7], and we set it to zero in our studies throughout the rest of this paper.

Comment on loop-induced production and decays

The one-loop mediated decays $Z' \rightarrow ZZ, Z\gamma, Zh$, etc., could provide an additional *a priori* opportunity to observe the Z' at hadron machines. The Furry [13] and Yang [14] theorems, and their extensions to decays into

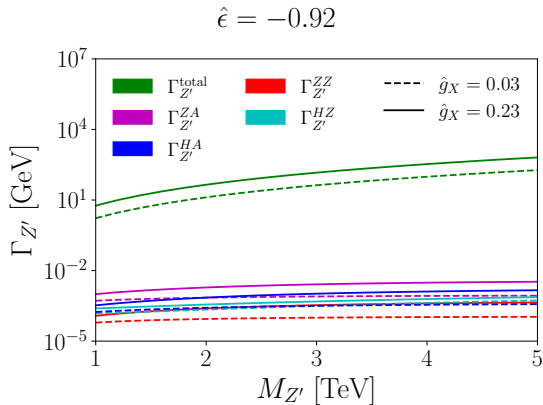


Figure 1: Representative loop-induced decays compared to the unsuppressed decay modes exploited further in this work.

massive final states [15], highly constrain the decay amplitudes (see also Refs. [16, 17]). They directly imply vanishing $Z' \rightarrow \gamma\gamma, gg$ decays. Non-vanishing amplitudes are controlled by the Z' axial vector couplings and the small mass splitting of the $SU(2)_L$ fermion doublet, which leads to an overall suppression of the loop-induced decays. To understand this more quantitatively, we have performed a full computation of representative loop-induced leading order decays and compare them to tree-level Z' decay phenomenology in the parameter region selected by flavour observations in Fig. 1. As is visible there, the loop-induced decays are typically two to three orders of magnitude below the dominant Z' decays. This also means that production mechanisms via gluon fusion (necessarily in association with additional jets to avoid symmetry selection rules) are highly suppressed.

3. Phenomenological opportunities at the HL-LHC and high precision lepton facilities

3.1. Z' at the HL-LHC and FCC-hh: muon signals and multi-jet cross checks

To obtain collider constraints on the model, we calculate the constraints from dedicated ‘bump-hunt’ searches across multiple final states. By a similar methodology, we acquire sensitivity estimates for future collider runs. Our analysis extends the work of Ref. [7], which focused on di-electron and di-muon final states, by incorporating di-jet resonance searches as well. The model is implemented in `FeynRules` [18, 19], which is subsequently interfaced with `MadGraph5_aMC@NLO` [20] via a `UFO` [21] model taken from Ref. [7]. We generate events for the production of the Z' via quark-antiquark annihilation (dominantly $b\bar{b}$), with subsequent decays into di-jet (including $b\bar{b}$

final states), di-muon, and di-electron final states, at a centre-of-mass energy $\sqrt{s} = 13$ TeV. We scan over a domain of values for $(\hat{g}_X, \hat{\epsilon})$ consistent with constraints from the previous literature [1, 7], for three benchmark mass values: $M_{Z'} = 2, 3, 4$ TeV. The 95% upper limits on the LHC cross-section times the branching ratios for di-jet, di-muon, and di-electron final states for the respective benchmark points are taken from recent LHC analyses [22–24] that provide model-independent constraints on potential new physics contributions at an integrated luminosity[‡] $\mathcal{L} = 139 \text{ fb}^{-1}$. To extrapolate these limits to estimate the High-Luminosity LHC (HL-LHC) sensitivity, we apply a $\sqrt{\mathcal{L}}$ scaling to the expected upper bound on the 95% CL production cross-section, which allows us to estimate the sensitivity of future HL-LHC runs at $\mathcal{L} = 3, 6 \text{ ab}^{-1}$ to the malaphoric $U(1)_{B_3-L_2}$ model. The collider sensitivities in the $(\hat{g}_X, \hat{\epsilon})$ parameter space for the different decay channels for the chosen mass benchmarks are shown on Fig. 2. The di-jet resonance searches provide the weakest exclusions and sensitivity of the channels we study and are not sensitive to much of the interesting parameter space. We extend our analysis to the FCC-hh ($\sqrt{s} = 100$ TeV) to evaluate its reach and to see if the di-jet channel will be of more use in such a context. We examine the FCC-hh sensitivity to di-jet resonance searches for the best-fit flavor constraints ($\hat{\epsilon} = -0.92$, $\hat{g}_X = (0.03, 0.23)$). Setting the best-fit flavour constraints, we scan over masses and generate cross-sections for $M_{Z'} = 20 - 40$ TeV. The

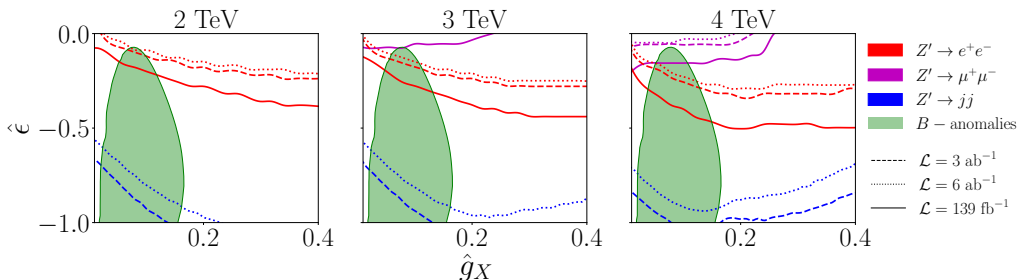


Figure 2: Bump-hunt bounds on the flavour-motivated malaphoric $B_3 - L_2$ model parameter space for $M_{Z'} = 2, 3, 4$ TeV. The region below each contour is sensitive to the 95% CL. 139 fb^{-1} curves are LHC bounds whereas the 3 and 6 ab^{-1} curves are the projected sensitivities at HL-LHC. $Z' \rightarrow \mu^+ \mu^-$ curves in the left panel are in the $\hat{\epsilon} > 0$ region.

[‡]Our results are consistent with those of Ref. [7], which found $M_{Z'} > 2.8$ TeV from current LHC di-muon searches, with sensitivity up to $M_{Z'} = 4.2$ TeV at the HL-LHC.

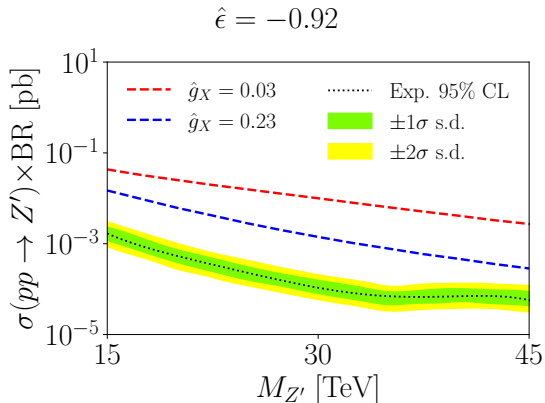


Figure 3: 95% CL sensitivity for a di-jet invariant mass bump hunt at the FCC-hh for 100 TeV collisions at an integrated luminosity $\mathcal{L} = 30 \text{ ab}^{-1}$. The entire 95% CL flavour-preferred parameter space can be probed.

resulting cross-sections, along with the 95% C.L. constraints on the projected upper bounds on di-jet resonance cross-sections at the FCC-hh [25], are shown in Figure 3. These demonstrate that the FCC-hh should easily be sensitive to all of the flavour-preferred parameter region. Since the di-lepton bump-hunt searches are more sensitive than those of di-jets, we may expect the FCC-hh to be sensitive to all three channels.

3.2. Z' at FCC- ee : (Non-)Oblique precision tests

A relatively likely follow-up to the LHC programme in the light of current ECFA discussions (see also [26]) and potentially imminent CEPC [27] decisions is an electron-positron collider, operating at the heavier SM particle mass thresholds, to produce abundant statistics for high precision Z and Higgs studies. The Z' model discussed in this work leads to modified corrections to EWPOs in comparison with the SM in two categories: oblique and non-oblique corrections, which we shall now discuss in turn.

Firstly, the kinetic mixing of the model implies characteristic oblique corrections [28] (see also [29, 30]). These flavour-universal modifications highlight BSM-induced changes to SM relations between the EWPOs for a chosen

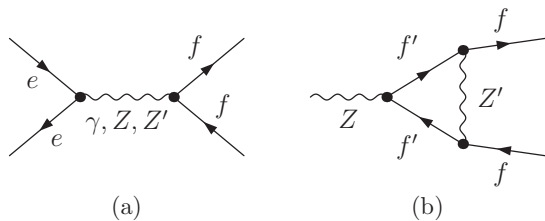


Figure 4: Representative Feynman diagrams contributing to the Z pole forward-backward asymmetry at e^+e^- colliders (a) and helicity asymmetries (b) at a comparable order in the $M_{Z'}^{-2}$ expansion.

electroweak input parameter set. The kinetic mixing modifies, e.g., the relation of the Z and W masses for the observed values of M_Z , the Fermi constant G_F and the fine-structure constant α_{EM} . This also becomes apparent from the matching of the model to the dimension-six Warsaw basis [31] as given in Ref. [1] with contributions to $O_{\Phi D}$ linked to the T parameter [32–35] (also feeding into the forward-backward asymmetry [36, 37]). Table 1 shows the largest contributions to representative quantities. The experimental numbers and pulls in the table are from *current* measurements and the increase in precision afforded by the FCC-ee would easily detect the size of such BSM effects.

Secondly, the tree-level exchange of the new heavy boson will induce a non-oblique deviation of the Z boson lineshape in exclusive e^+e^- collisions by probing the off-shell Z' contribution and its specific couplings to, e.g., b quarks and muons. The dominant effect is driven by the Z' exchange interfering with the SM amplitude (e.g. Fig. 4(a)). The relevant effects are $\sim (\Gamma_Z/M_{Z'})^2 \ll 1$ suppressed ($\Gamma_Z \simeq 2.4$ GeV is the SM width of the Z boson) and therefore require very high precision to obtain competitive bounds, highlighting the FCC-ee as the relevant environment to look for such effects. The expected precision of FCC-ee measurements also motivates the consideration of loop-suppressed topologies. For measurements on the Z pole, the most relevant ones are the vertex corrections depicted in Fig. 4(b). As they are directly sensitive to the initial and final state lepton and quark flavours, they provide a further non-oblique avenue to constrain the malaporphic $B_3 - L_2$ model.[§] The new ultraviolet singularities sourced by the Z' vertex correction cancel against the fermion wave function corrections in the on-shell scheme, rendering the virtual corrections shown in Fig. 4(b) manifestly ultraviolet finite for any value of the off-shell Z boson current. Measurable quantities can be derived from the latter by considering the helicity asymmetry ratios of the $Z \rightarrow f\bar{f}$ pole pseudo-observable,

$$A_{\text{LR}}^f = \frac{\Gamma(Z \rightarrow f_L \bar{f}_R) - (R \leftrightarrow L)}{\Gamma(Z \rightarrow f_L \bar{f}_R) + (R \leftrightarrow L)} = \frac{(\frac{1}{2} - |Q_f|s_w^2)^2 - Q_f^2 s_w^4}{(\frac{1}{2} - |Q_f|s_w^2)^2 + Q_f^2 s_w^4} + \mathcal{O}\left(\frac{m_f^2}{M_Z^2}\right), \quad (5)$$

[§]Working in the on-shell scheme, $Z - Z'$ mixing is absent, and additional box topologies are suppressed with respect to the Z boson Breit-Wigner enhancement. In the following, we will not further comment on these effects but interest ourselves in the relative importance of universal and non-universal corrections.

Observable	experiment	$B_3 - L_2$	SM-pull
M_W/GeV	80.3795 ± 0.01210	80.3646	1.60
A_{LR}^{ee}	0.15132 ± 0.00193	0.14916	1.53

Table 1: EWPOs as calculated by `flavio2.3.3` and `smelli2.3.2` [38] whose SM-pull is larger than unity for the best-fit $B_3 - L_2$ point and $M_X = 3$ TeV, where SM-pull= $|\text{SM prediction} - (B_3 - L_2 \text{ prediction})|/\text{uncertainty}$.

	A_{LR}^b	A_{LR}^c	A_{LR}^τ	A_{LR}^μ	A_{LR}^e
SM Leading Order	0.943	0.941	0.216	0.216	0.216
SM NLO electroweak	-0.007	-0.031	-0.075	-0.075	-0.075

Table 2: Predicted helicity asymmetries in the SM at one-loop electroweak precision. See the main body of text for details.

(at leading electroweak order) where m_f is the fermion mass and Q_f is the electric charge of fermionic field f . It is known that these observables, which are connected to the $e^+e^- \rightarrow Z \rightarrow f\bar{f}$ Z -pole forward-backward asymmetry via [39]

$$A_{\text{FB}}^f = \frac{3}{4} A_{\text{LR}}^e A_{\text{LR}}^f, \quad (6)$$

are susceptible to radiative corrections [40–42]. We consider the Z' -induced corrections to these observables for different relevant final states f in the following.

The Z' -related corrections should also be compared to the expected size of

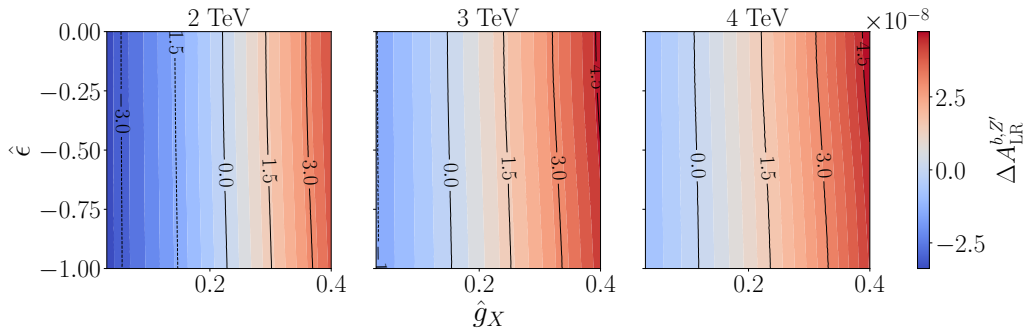


Figure 5: Helicity asymmetry $\Delta A_{\text{LR}}^{b,Z'}$ modifications induced by the one-loop Z' contribution such as that depicted in Fig. 4b. Note the tiny scaling factor above the colour bar on the far right.

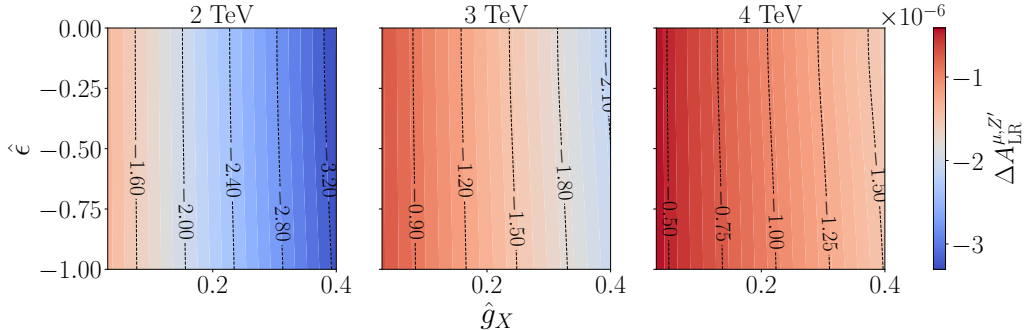


Figure 6: Muon helicity asymmetry $\Delta A_{\text{LR}}^{\mu, Z'}$ induced by the one-loop Z' contribution such as that depicted in Fig. 4b. Note the scaling factor above the colour bar on the far right.

the SM weak corrections to qualitatively understand their relevance. Similar to the computation of the Z' insertion, we have performed a calculation of A_{LR}^f in the SM[¶]. The results^{||} are shown in Table 2. The comparison clearly indicates that the radiative vertex effects induced by the Z' are small in the parameter region that the HL-LHC explores.

In the limit of $m_b, M_Z \ll M_{Z'}$ we find that in e.g. the $Z \rightarrow b\bar{b}$ decay the $\mathcal{O}(\epsilon)$ term (for demonstration purposes) is

$$\Delta A_{\text{LR}}^{b, Z'} \simeq -\frac{\epsilon g_X^2}{9\pi^2} \frac{s_w^5 (3 - 2s_w^2)^2}{(9 - 12s_w^2 + 8s_w^4)^2} \frac{M_Z^2}{M_{Z'}^2} \left(6 \log \left[\frac{m_b^2}{M_{Z'}^2} \right] - 1 \right) \quad (7)$$

at one-loop order. This turns out to be small due to the loop suppression factor and the $M_Z^2/M_{Z'}^2 \ll 1$ factor. Full one-loop results are presented in Figs. 5 and 6 for the bottom quark and the muon, respectively.

In contrast, the interference of the the tree-level Z' with the SM amplitude, the forward-backward asymmetry on the Z resonance (at $M_{Z'} = 2$ TeV for example) is $\Delta A_{\text{FB}}^{bb, Z'} \simeq 3.8 \times 10^{-7}$ for the $b\bar{b}$ mode for the best fit point.

A scan over the parameter domain of interest is presented in Figs. 7 and 8, for the b quark and the muon for three benchmark points with $M_{Z'} = 2, 3, 4$ TeV. The flavour-specific contributions discussed above also

[¶]From now on, we use input parameters $\alpha_{\text{EM}} \simeq 1/132.50$, $M_W \simeq 80.42$ GeV, and $M_Z \simeq 91.18$ GeV.

^{||}The soft photon contribution is regularised with an effective photon mass according to Ref. [43] that cancels against the real emission contribution through the Bloch-Nordsiek [44] or Kinoshita-Lee-Nauenberg theorem [45, 46]. As the photon emission is non-chiral, its contributions cancel in Eq. (5) except for a finite remainder (see also [47]).

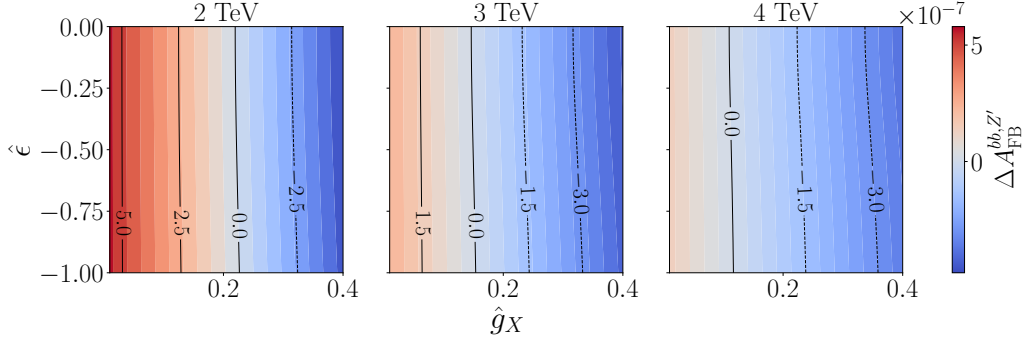


Figure 7: Forward-backward asymmetry $\Delta A_{\text{FB}}^{bb,Z'}$ modifications induced by the malaphoric $B_3 - L_2 Z'$ interfering with the Z lineshape. Note the scaling factor above the colour bar on the right.

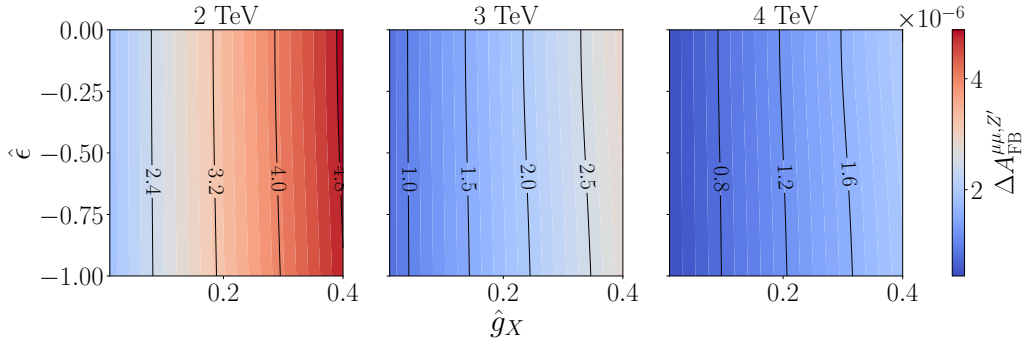


Figure 8: Forward-backward asymmetry $\Delta A_{\text{FB}}^{\mu\mu,Z'}$ modifications induced by the malaphoric $B_3 - L_2 Z'$ tree-level exchange interfering with the Z lineshape. Note the tiny scaling factor above the colour bar on the right.

compare unfavourably to the projected TeraZ sensitivity [48–50] (e.g., the estimated uncertainties on A_{LR}^b and A_{LR}^μ are of the order $\mathcal{O}(10^{-5})$). While the FCC-ee would be able to constrain the model through mixing effect related EWPOs (see again Tab. 1), more direct, model-specific modifications from loop correction modifications would be unlikely to provide any additional sensitivity. An FCC-hh, on the other hand, as shown before, would be sensitive to the whole across the malaphoric $B_3 - L_2$ model’s flavour-preferred parameter space.

4. Conclusions

Flavour measurements inform the search for physics BSM, as do direct exclusion limits from direct new particle searches at the highest attainable collider energies. Current measurements in B -meson decays that involve the $b \rightarrow s$ transition show a significant tension with state-of-the-art SM expectations [11, 51]. We take this as motivation to consider a particular scenario (the malaphoric $B_3 - L_2$ model) that dynamically explains neutral current anomalies in the B sector to contextualise the anomalies' discovery implications at present and future colliders.

The HL-LHC has the ability to increase sensitivity to the model somewhat beyond current limits. The oblique corrections have BSM changes to them that would be detectable at the FCC-ee [1]. FCC-ee non-oblique precision tests, chiefly those informed by characteristic vertex corrections, would unlikely probe the flavour-preferred region of parameter space beyond this. We have further shown that the FCC-hh would be sensitive to all of the flavour-preferred parameter space, even in the less sensitive di-jets mode. In the case that the HL-LHC makes no BSM discovery, at the FCC-hh one could check the correlated signal strengths of equal mass di-electron, di-muon and di-jet bumps in order to further check and constrain the model.

Acknowledgements — This work has been partially supported by the Science Technology and Facilities Council consolidated grants ST/T000694/1 and ST/X000664/1. B.C.A. thanks the Cambridge Pheno Working Group for helpful discussions and the Glasgow Particle Physics Theory group for hospitality enjoyed while part of this work was carried out. W.N. thanks Mario Fernandez Navarro for fruitful discussions. C.E. acknowledges partial support by the Leverhulme Trust Research Project RPG-2021-031 and Research Fellowship RF-2024-300\9. C.E. is further supported by the Institute for Particle Physics Phenomenology Associateship Scheme. W.N. is funded by a University of Glasgow College of Science and Engineering Fellowship.

References

- [1] B. Allanach and N. Gubernari, *Malaphoric Z' models for $b \rightarrow sl^+\ell^-$ anomalies*, *Eur. Phys. J. C* **85** (2025) 2, [[arXiv:2409.06804](https://arxiv.org/abs/2409.06804)].
- [2] M. Bordone, A. Greljo, and D. Marzocca, *Exploiting dijet resonance searches for flavor physics*, *JHEP* **08** (2021) 036, [[arXiv:2103.10332](https://arxiv.org/abs/2103.10332)].

- [3] S. Bißmann, J. Erdmann, C. Grunwald, G. Hiller, and K. Kröninger, *Constraining top-quark couplings combining top-quark and \mathbf{B} decay observables*, *Eur. Phys. J. C* **80** (2020), no. 2 136, [[arXiv:1909.13632](#)].
- [4] C. Grunwald, G. Hiller, K. Kröninger, and L. Nollen, *More synergies from beauty, top, Z and Drell-Yan measurements in SMEFT*, *JHEP* **11** (2023) 110, [[arXiv:2304.12837](#)].
- [5] C. Englert, C. Mayer, W. Naskar, and S. Renner, *Doubling down on down-type diquarks*, [arXiv:2410.00952](#).
- [6] J. Davighi, *In Search of an Invisible Z'* , [arXiv:2412.07694](#).
- [7] B. Allanach, *Constraints on the malaporphic $B_3 - L_2$ model from di-lepton resonance searches at the LHC*, [arXiv:2412.01956](#).
- [8] M. Algueró, A. Biswas, B. Capdevila, S. Descotes-Genon, J. Matias, and M. Novoa-Brunet, *To (b)e or not to (b)e: no electrons at LHCb*, *Eur. Phys. J. C* **83** (2023), no. 7 648, [[arXiv:2304.07330](#)].
- [9] B. Allanach and A. Mullin, *Plan B: new Z' models for $b \rightarrow s\ell^+\ell^-$ anomalies*, *JHEP* **09** (2023) 173, [[arXiv:2306.08669](#)].
- [10] N. Gubernari, M. Reboud, D. van Dyk, and J. Virto, *Improved theory predictions and global analysis of exclusive $b \rightarrow s\mu^+\mu^-$ processes*, *JHEP* **09** (2022) 133, [[arXiv:2206.03797](#)].
- [11] **HPQCD** Collaboration, W. G. Parrott, C. Bouchard, and C. T. H. Davies, *Standard Model predictions for $B \rightarrow K\ell^+\ell^-$, $B \rightarrow K\ell_1^-\ell_2^+$ and $B \rightarrow K\nu\bar{\nu}$ using form factors from $N_f = 2 + 1 + 1$ lattice QCD*, *Phys. Rev. D* **107** (2023), no. 1 014511, [[arXiv:2207.13371](#)]. [Erratum: *Phys.Rev.D* 107, 119903 (2023)].
- [12] M. Ciuchini, M. Fedele, E. Franco, A. Paul, L. Silvestrini, and M. Valli, *Constraints on lepton universality violation from rare B decays*, *Phys. Rev. D* **107** (2023), no. 5 055036, [[arXiv:2212.10516](#)].
- [13] W. H. Furry, *A Symmetry Theorem in the Positron Theory*, *Phys. Rev.* **51** (1937) 125–129.
- [14] C.-N. Yang, *Selection Rules for the Dematerialization of a Particle Into Two Photons*, *Phys. Rev.* **77** (1950) 242–245.

- [15] W.-Y. Keung, I. Low, and J. Shu, *Landau-Yang Theorem and Decays of a Z' Boson into Two Z Bosons*, *Phys. Rev. Lett.* **101** (2008) 091802, [[arXiv:0806.2864](#)].
- [16] L. Michaels and F. Yu, *Probing new $U(1)$ gauge symmetries via exotic $Z \rightarrow Z'\gamma$ decays*, *JHEP* **03** (2021) 120, [[arXiv:2010.00021](#)].
- [17] J. Davighi, *Anomalous Z' bosons for anomalous B decays*, *JHEP* **08** (2021) 101, [[arXiv:2105.06918](#)].
- [18] N. D. Christensen and C. Duhr, *FeynRules - Feynman rules made easy*, *Comput. Phys. Commun.* **180** (2009) 1614–1641, [[arXiv:0806.4194](#)].
- [19] A. Alloul, N. D. Christensen, C. Degrande, C. Duhr, and B. Fuks, *FeynRules 2.0 - A complete toolbox for tree-level phenomenology*, *Comput. Phys. Commun.* **185** (2014) 2250–2300, [[arXiv:1310.1921](#)].
- [20] J. Alwall, R. Frederix, S. Frixione, V. Hirschi, F. Maltoni, O. Mattelaer, H. S. Shao, T. Stelzer, P. Torrielli, and M. Zaro, *The automated computation of tree-level and next-to-leading order differential cross sections, and their matching to parton shower simulations*, *JHEP* **07** (2014) 079, [[arXiv:1405.0301](#)].
- [21] C. Degrande, C. Duhr, B. Fuks, D. Grellscheid, O. Mattelaer, and T. Reiter, *UFO - The Universal FeynRules Output*, *Comput. Phys. Commun.* **183** (2012) 1201–1214, [[arXiv:1108.2040](#)].
- [22] E. Maguire, L. Heinrich, and G. Watt, *HEPData: a repository for high energy physics data*, *J. Phys. Conf. Ser.* **898** (2017), no. 10 102006, [[arXiv:1704.05473](#)].
- [23] **ATLAS** Collaboration, G. Aad et al., *Search for high-mass dilepton resonances using 139 fb^{-1} of pp collision data collected at $\sqrt{s} = 13 \text{ TeV}$ with the ATLAS detector*, *Phys. Lett. B* **796** (2019) 68–87, [[arXiv:1903.06248](#)].
- [24] **CMS** Collaboration, A. M. Sirunyan et al., *Search for high mass dijet resonances with a new background prediction method in proton-proton collisions at $\sqrt{s} = 13 \text{ TeV}$* , *JHEP* **05** (2020) 033, [[arXiv:1911.03947](#)].

- [25] C. Helsens, D. Jamin, M. L. Mangano, T. G. Rizzo, and M. Selvaggi, *Heavy resonances at energy-frontier hadron colliders*, *Eur. Phys. J. C* **79** (2019) 569, [[arXiv:1902.11217](#)].
- [26] **European Strategy Group** Collaboration, H. Abramowicz et al., *2020 Update of the European Strategy for Particle Physics*. CERN Council, Geneva, 2020.
- [27] **CEPC Study Group** Collaboration, W. Abdallah et al., *CEPC Technical Design Report: Accelerator, Radiat. Detect. Technol. Methods* **8** (2024), no. 1 1–1105, [[arXiv:2312.14363](#)]. [Erratum: *Radiat.Detect.Technol.Methods* None, (2024)].
- [28] B. Holdom, *Two $U(1)$'s and Epsilon Charge Shifts*, *Phys. Lett. B* **166** (1986) 196–198.
- [29] E. Weihs and J. Zurita, *Dark Higgs Models at the 7 TeV LHC*, *JHEP* **02** (2012) 041, [[arXiv:1110.5909](#)].
- [30] S. Y. Choi, C. Englert, and P. M. Zerwas, *Multiple Higgs-Portal and Gauge-Kinetic Mixings*, *Eur. Phys. J. C* **73** (2013) 2643, [[arXiv:1308.5784](#)].
- [31] B. Grzadkowski, M. Iskrzynski, M. Misiak, and J. Rosiek, *Dimension-Six Terms in the Standard Model Lagrangian*, *JHEP* **10** (2010) 085, [[arXiv:1008.4884](#)].
- [32] G. Altarelli and R. Barbieri, *Vacuum polarization effects of new physics on electroweak processes*, *Phys. Lett. B* **253** (1991) 161–167.
- [33] M. E. Peskin and T. Takeuchi, *A New constraint on a strongly interacting Higgs sector*, *Phys. Rev. Lett.* **65** (1990) 964–967.
- [34] B. Grinstein and M. B. Wise, *Operator analysis for precision electroweak physics*, *Phys. Lett. B* **265** (1991) 326–334.
- [35] G. Altarelli, R. Barbieri, and S. Jadach, *Toward a model independent analysis of electroweak data*, *Nucl. Phys. B* **369** (1992) 3–32. [Erratum: *Nucl.Phys.B* 376, 444 (1992)].
- [36] M. E. Peskin and T. Takeuchi, *Estimation of oblique electroweak corrections*, *Phys. Rev. D* **46** (1992) 381–409.

- [37] C. P. Burgess, S. Godfrey, H. Konig, D. London, and I. Maksymyk, *Model independent global constraints on new physics*, *Phys. Rev. D* **49** (1994) 6115–6147, [[hep-ph/9312291](#)].
- [38] J. Aebischer, J. Kumar, P. Stangl, and D. M. Straub, *A Global Likelihood for Precision Constraints and Flavour Anomalies*, *Eur. Phys. J. C* **79** (2019), no. 6 509, [[arXiv:1810.07698](#)].
- [39] M. E. Peskin and D. V. Schroeder, *An Introduction to quantum field theory*. Addison-Wesley, Reading, USA, 1995.
- [40] D. Y. Bardin, S. Riemann, and T. Riemann, *Electroweak One Loop Corrections to the Decay of the Charged Vector Boson*, *Z. Phys. C* **32** (1986) 121–125.
- [41] D. Y. Bardin, P. Christova, M. Jack, L. Kalinovskaya, A. Olchevski, S. Riemann, and T. Riemann, *ZFITTER v.6.21: A Semianalytical program for fermion pair production in e^+e^- annihilation*, *Comput. Phys. Commun.* **133** (2001) 229–395, [[hep-ph/9908433](#)].
- [42] **Gfitter Group** Collaboration, M. Baak, J. Cúth, J. Haller, A. Hoecker, R. Kogler, K. Mönig, M. Schott, and J. Stelzer, *The global electroweak fit at NNLO and prospects for the LHC and ILC*, *Eur. Phys. J. C* **74** (2014) 3046, [[arXiv:1407.3792](#)].
- [43] G. 't Hooft and M. J. G. Veltman, *Scalar One Loop Integrals*, *Nucl. Phys. B* **153** (1979) 365–401.
- [44] F. Bloch and A. Nordsieck, *Note on the Radiation Field of the electron*, *Phys. Rev.* **52** (1937) 54–59.
- [45] T. Kinoshita, *Mass singularities of Feynman amplitudes*, *J. Math. Phys.* **3** (1962) 650–677.
- [46] T. D. Lee and M. Nauenberg, *Degenerate Systems and Mass Singularities*, *Phys. Rev.* **133** (1964) B1549–B1562.
- [47] S. Catani and M. H. Seymour, *A General algorithm for calculating jet cross-sections in NLO QCD*, *Nucl. Phys. B* **485** (1997) 291–419, [[hep-ph/9605323](#)]. [Erratum: *Nucl.Phys.B* 510, 503–504 (1998)].

- [48] N. Alipour Tehrani et al., *FCC-ee: Your Questions Answered*, in *CERN Council Open Symposium on the Update of European Strategy for Particle Physics* (A. Blondel and P. Janot, eds.), 6, 2019. [arXiv:1906.02693](#).
- [49] A. Blondel et al., *Polarization and Centre-of-mass Energy Calibration at FCC-ee*, [arXiv:1909.12245](#).
- [50] A. Blondel and P. Janot, *FCC-ee overview: new opportunities create new challenges*, *Eur. Phys. J. Plus* **137** (2022), no. 1 92, [[arXiv:2106.13885](#)].
- [51] N. Gubernari, M. Reboud, D. van Dyk, and J. Virto, *Improved theory predictions and global analysis of exclusive $b \rightarrow s\mu^+\mu^-$ processes*, *JHEP* **09** (2022) 133, [[arXiv:2206.03797](#)].